Environmental Science
Processes & Impacts

PAPER

View Article Online
View Journal | View Issue

Cite this: *Environ. Sci.: Processes Impacts*, 2017, **19**, 1414

Environmental photochemistry of dienogest: phototransformation to estrogenic products and increased environmental persistence *via* reversible photohydration†

Nicholas C. Pflug,[a] Madeline K. Hankard,[b] Stephanie M. Berg,[b] Meghan O'Connor,[c] James B. Gloer,[a] Edward P. Kolodziej,[de] David M. Cwiertny*[c] and Kristine H. Wammer*[b]

Potent trienone and dienone steroid hormones undergo a coupled photohydration (in light)-thermal dehydration (in dark) cycle that ultimately increases their environmental persistence. Here, we studied the photolysis of dienogest, a dienone progestin prescribed as a next-generation oral contraceptive, and used high resolution mass spectrometry and both 1D and 2D nuclear magnetic resonance spectroscopy to identify its phototransformation products. Dienogest undergoes rapid direct photolysis ($t_{1/2}$ ~ 1–10 min), forming complex photoproduct mixtures across the pH range examined (pH 2 to 7). Identified products include three photohydrates that account for ~80% of the converted mass at pH 7 and revert back to parent dienogest in the absence of light. Notably, we also identified two estrogenic compounds produced *via* the A-ring aromatization of dienogest, evidence for a photochemically-induced increase in estrogenic activity in product mixtures. These results imply that dienogest will undergo complete and facile photolytic transformation in sunlit surface water, yet exhibit greater environmental persistence than might be anticipated by inspection of kinetic rates. Photoproduct mixtures also include transformation products with different nuclear receptor binding capabilities than the parent compound dienogest. These outcomes reveal a dynamic fate and biological risk profile for dienogest that must also take into account the composition and endocrine activity of its transformation products. Collectively, this study further illustrates the need for more holistic regulatory, risk assessment, and monitoring approaches for high potency synthetic pharmaceuticals and their bioactive transformation products.

Received 28th July 2017
Accepted 5th October 2017

DOI: 10.1039/c7em00346c

rsc.li/espi

Environmental significance

For bioactive chemical classes, it is often assumed that environmental transformation eliminates associated ecosystem risks. Here, we show that photolysis of dienogest, a potent and widely prescribed pharmaceutical steroid, can yield photohydrates that revert back to parent in the dark, in addition to mixtures of known, bioactive steroidal transformation products. This work calls attention to the likely persistence of dienogest through product-to-parent reversion and formation of bioactive transformation products in sunlit surface waters or engineered photochemical systems, some of which may have adverse implications for ecosystem health.

Introduction

According to the EPA's Contaminant Candidate List (CCL), steroid hormones are likely to be among the first emerging pollutant classes regulated in drinking water because of their ubiquitous occurrence and potency as endocrine-active compounds.[1–4] Their high potency implies potential reproductive, developmental, and homeostatic effects at nanomolar (nM) or even sub-nM concentrations in exposed aquatic organisms; concentrations that are near to, and sometimes even below, those expected in contaminated surface waters.[5–8] Structurally, several of the most potent synthetic steroids used as human or

[a]*Department of Chemistry, University of Iowa, Iowa City, IA 52242, USA*
[b]*Department of Chemistry, University of St. Thomas, 2115 Summit Avenue, St. Paul, MN 55105, USA. E-mail: khwammer@stthomas.edu; Tel: +1-651-962-5574*
[c]*Department of Civil and Environmental Engineering, University of Iowa, 4136 Seamans Center, Iowa City, IA 52242, USA. E-mail: david-cwiertny@uiowa.edu; Tel: +1-319-335-1401*
[d]*Interdisciplinary Arts and Sciences, University of Washington, Tacoma, WA 98402, USA*
[e]*Department of Civil and Environmental Engineering, University of Washington, Seattle, WA 98195, USA*

† Electronic supplementary information (ESI) available. See DOI: 10.1039/c7em00346c

agricultural pharmaceuticals incorporate dienone or trienone functionalities into their structures, including 17β-trenbolone, altrenogest, dienedione, and dienogest. Such trienone or dienone functionalities are specifically chosen because the resulting coplanar steroid structure increases receptor binding affinity and thus increases ligand potency of the pharmaceutical.[9]

We discovered that the incorporation of trienone and dienone functionalities into synthetic pharmaceuticals holds unexpected implications for their environmental fate and reactivity, particularly with respect to photolysis.[10–14] Trienone and dienone conjugated π-bond systems are thermodynamically favorable relative to their phototransformation products with disrupted or reduced conjugation.[10] During irradiation with natural sunlight, we demonstrated a coupled photohydration (in light)-thermal dehydration (in dark) mechanism for this compound family that results in reversion of less conjugated transformation products back to their more conjugated parent structures.[13] This photoproduct-to-parent reversion cycle increases persistence of dienone and trienone steroids, and maintains contaminant hazard in the aquatic system despite the appearance of attenuation.[13] In fact, for these families of synthetic steroids for which photolysis is often presumed to be the fastest environmental degradation pathway, mixture potency typically only decreases in proportion to the minor yields of phototransformation products not subject to thermal dehydration, assuming these products are not biologically active (which may not always be true).[10]

This behavior, first described for 17β-trenbolone and related metabolites of trenbolone acetate,[13] provides another clear example of retained bioactivity and conservation of critical pharmacophore attributes during environmental reactions of high potency pharmaceuticals.[15,16] Additional examples in the literature include increased estrogenicity of oxidation products of ethinyl estradiol,[17] persistent estrogen receptor (ER) activity after chlorination of 17β-estradiol,[18] persistent glucocorticoid receptor (GR) activity after chlorination of cortisol,[19] and conversion of testosterone to boldenone *via* microbial transformation,[20] among other reports.[11] Another example occurs for the trienone progestin altrenogest, widely used to synchronize estrus in swine production.[21,22] Altrenogest very rapidly photolyzes (∼30 s half-life) to form a unique cycloaddition photoproduct containing a dienone functionality that is prone to subsequent photohydration–thermal dehydration cycling.[14] Further, although the cycloaddition product is expected to demonstrate potency for the progesterone receptor (PR), we also demonstrated its affinity for the androgen receptor (AR), implying otherwise unexpected bioactivities and risks for biological endpoints (*e.g.*, nuclear receptor binding) in exposed organisms.[14]

Amidst increasing scrutiny of the environmental fate of highly potent synthetic progestins,[8] we herein explore the coupled photohydration–thermal dehydration of the dienone pharmaceutical dienogest. Dienogest (DNG) is a synthetic progestin approved for use as an oral contraceptive and treatment of endometriosis that is 10-fold more potent than levonorgestrel, commonly used as an emergency contraceptive progestin (*i.e.*, plan B).[23–25] Both of these applications rely upon daily doses of ∼1–2 mg of active compound.[24,26] Also, metabolism of DNG in microbially active systems[27] has yielded metabolites with an aromatic A-ring, a structural feature typically resulting in significant estrogenic activity. This suggest that other transformation mechanisms, such as photolysis, may also form estrogenic transformation products.

Given these observations, we wanted to elucidate the structure and stability of DNG phototransformation products. In laboratory experiments, we evaluated the impacts of environmental factors (*i.e.*, pH and dissolved oxygen concentrations) on both the rate and extent of DNG photolysis and transformation product stability. Using semi-preparative high performance liquid chromatography (HPLC), ultraviolet-visible (UV-VIS) spectrophotometry, high resolution mass spectrometry (HRMS) and nuclear magnetic resonance spectroscopy (NMR), we then identified major transformation products. Outcomes of this work should improve predictions of the environmental persistence and fate of DNG, while also guiding future occurrence studies for novel or bioactive transformation products of potent synthetic steroids.

Materials and methods

Reagents

Photolysis experiments used dienogest (Sigma; ≥98% HPLC), anhydrous potassium phosphate monobasic (KH_2PO_4; RPI; ACS grade) and deionized water (Millipore, Q-Grad 2). Liquid–liquid extractions were performed with chloroform (Fisher Scientific; ACS grade). HPLC analysis used mixtures of deionized water (Millipore, Q-Grad 2) and acetonitrile (Fisher Scientific; ACS HPLC grade) as the mobile phase.

Photolysis experiments

The majority of experiments were conducted using a commercially available 1000 W xenon arc lamp (Newport Corporation). The light was first passed through a water filter to remove IR radiation, reflected off a 90° full reflectance beam turning mirror, and then passed through an AM 1.5 filter and a 305 nm long-pass filter to generate a spectrum of light more closely resembling that available at the earth's surface. Lamp irradiance (1660 W m^{-2}) for wavelengths greater than 305 nm was measured with a spectroradiometer (ILT950; International Light Technologies, Peabody, MA). Unless noted, all photochemical experiments were conducted in a water-jacketed, borosilicate photoreactor (37 mm inner diameter × 67 mm depth for a nominal volume of ∼50 mL; Chemglass), whose contents were mixed *via* a magnetic stirrer and stir plate. Reactors were loaded with 20 mL of 5 mM potassium phosphate buffer (pH 2, 5 or 7) and an initial aqueous DNG concentration of 25 μM (∼8 mg L^{-1}; from freshly prepared 10 mM methanolic stock solutions). The system temperature (∼20 °C) was held constant *via* a recirculating water bath. Upon irradiation, samples were withdrawn periodically over time to monitor the concentration of the parent DNG and any detectable transformation products *via* HPLC analysis.

A subset of "scaled-up" experiments requiring large volumes to facilitate product identification were conducted using an Atlas Suntest CPS + solar simulator. The solar simulator was equipped with a xenon lamp and an Atlas UV Suntest filter, and provided an emission spectrum accurately simulating that of natural sunlight with an irradiance of 500 W m^{-2} (or ~2/3 of the anticipated irradiance at summer solar noon at mid-latitudes). Borosilicate beakers (1 L) were loaded with 500 mL of 5 mM potassium phosphate buffer (pH 2, 5 or 7) and an initial aqueous DNG concentration of 100 μM (~31 mg L^{-1}; from freshly prepared 10 mM methanolic stock solutions). Upon irradiation, samples were withdrawn periodically over time to monitor the concentration of the parent DNG and any detectable transformation products *via* HPLC analysis. Samples were then extracted into chloroform and concentrated to a residue by a stream of compressed air before further chemical analysis.

For photolysis kinetics, the same solar simulator described above was used. DNG solutions were placed in quartz test tubes and the test tubes were held at a 45° angle. Photolysis time varied between experiments, and samples were taken periodically. At the conclusion of photolysis experiments, aliquots of the photolyzed solution were placed in amber vials and stored in the dark for up to five days, or until no more regeneration of DNG was observed. Samples from these dark regeneration experiments were analyzed once to twice a day to monitor the reaction progress.

Analytical methods

High performance liquid chromatography. Samples were analyzed with an Agilent 1200 series HPLC-Diode Array Detector (DAD) system. The method used either an Agilent Zorbax Eclipse XDB-C_{18} (4.6 × 150 mm, 3.5 μm) or Agilent PREP-C_{18} Scalar (4.6 × 150 mm, 5 μm) column with acetonitrile/water gradient elution (1 mL min^{-1}) and scanning 200–400 nm wavelength detection. HPLC separations were performed using a Beckman System Gold instrument with a model 166P VWD connected to a 128P solvent module, with acetonitrile/water gradient elution (2 mL min^{-1}), 250 nm wavelength detection, and a Restek Ultra C_8 semi-preparative (10 × 250 mm, 5 μm) column.

Nuclear magnetic resonance spectroscopy. ^{1}H NMR, homonuclear correlation spectroscopy (COSY), heteronuclear single quantum coherence (HSQC), heteronuclear multiple bond correlation (HMBC), and nuclear overhauser effect spectroscopy (NOESY) spectra were recorded using a Bruker AVANCE-600 spectrometer using $CDCl_3$ as the solvent. Chemical shift values were referenced to the residual solvent signals (δ_H/δ_C, 7.26/77.2). All NMR data were processed using Bruker Topspin 3.5 software.

High resolution electrospray ionization time-of-flight mass spectrometry (HR-ESI-TOFMS). HR-ESI-TOFMS data were obtained using a Waters Premier Q-TOF instrument, the same chromatographic method as listed above (HPLC-DAD) with the addition of a 0.1% formic acid solution and collected using a reference standard of leu-enkaphalin and positive electrospray ionization over a mass range of 120–1000 Da under the following instrument parameters: 20 μL injection volume; 2.8 kV capillary, 35.0 V sampling cone, 4.0 V extraction cone and 2.0 V ion guide voltages; 110 °C source temperature, and 400 °C desolvation temperature.

High resolution electron ionization time-of-flight mass spectrometry (HR-EI-TOFMS). HR-EI-TOFMS data were obtained using a Waters Premier Q-TOF instrument with direct injection and collected using a reference standard of leu-enkaphalin and electron ionization over a mass range of 120–1000 Da.

Molecular modeling. Spartan 2016 (V2.0.3) was used to create energy minimized models of certain transformation products to guide stereochemical assignments. In brief, structures were drawn and energy minimized, followed by an equilibrium conformer calculation using MMFF molecular mechanics and Monte-Carlo searching.

Results and discussion

Direct photolysis and regeneration of dienogest

DNG undergoes rapid direct photolysis across pH 2 to 7. Measured pseudo-first-order rate coefficients, or k_{obs} values, were estimated from linear regression analyses of semi-log plots of DNG concentration as a function of time (shown in Fig. S1 of the ESI†). Experiments revealed the following pH-dependent reactivity trend, where values in parentheses indicate half-lives [$t_{1/2}$ values = $\ln(2)/k_{obs}$] with standard deviations from three replicate experiments: pH 7 ($t_{1/2} \sim 0.94 \pm 0.05$ min) ~ pH 5 ($t_{1/2} \sim 1.1 \pm 0.1$ min) >> pH 2 ($t_{1/2} \sim 10.6 \pm 0.8$ min) (Fig. 1A).

Compared to other steroids we have previously investigated, the rate of DNG direct photolysis is most similar to that of the synthetic progestin altrenogest (ALT; $t_{1/2} \sim 30$ s),[14] with both ALT and DNG reacting markedly faster than the synthetic growth promoters trenbolone acetate (and its metabolites; $t_{1/2} \sim$ 20–30 min) and melengestrol acetate (and its hydrolysis product; $t_{1/2} \sim 50$ min).[12] Therefore, it is reasonable to expect that DNG will undergo complete and facile photolytic transformation in sunlit surface waters or engineered photochemical systems (*e.g.*, UV disinfection systems). We note that the presence or absence of oxygen in the experimental system, which affected ALT photo-isomerization,[14] had little-to-no observable impact on DNG photolysis (see Fig. S2†).

As observed previously,[13] DNG was regenerated from photoproduct mixtures in the dark across the range of pH values considered (Fig. 1B), even after complete DNG phototransformation (*i.e.*, to levels below our limit of analytical detection). For trenbolone acetate metabolites, this product-to-parent reversion proceeds *via* light-mediated water addition (*i.e.*, photohydration) across its trienone moiety followed by acid- or base-catalyzed dehydration in the dark to regenerate the parent compound.[13] A similar mechanism for DNG is consistent with our data. The extended conjugation (dienone, $\lambda_{max} \sim$ 310 nm) of DNG should render it susceptible to photohydration *via* direct photolysis and subsequent thermal dehydration. Accordingly, we suspected one or more photohydrates to be among the primary phototransformation products.

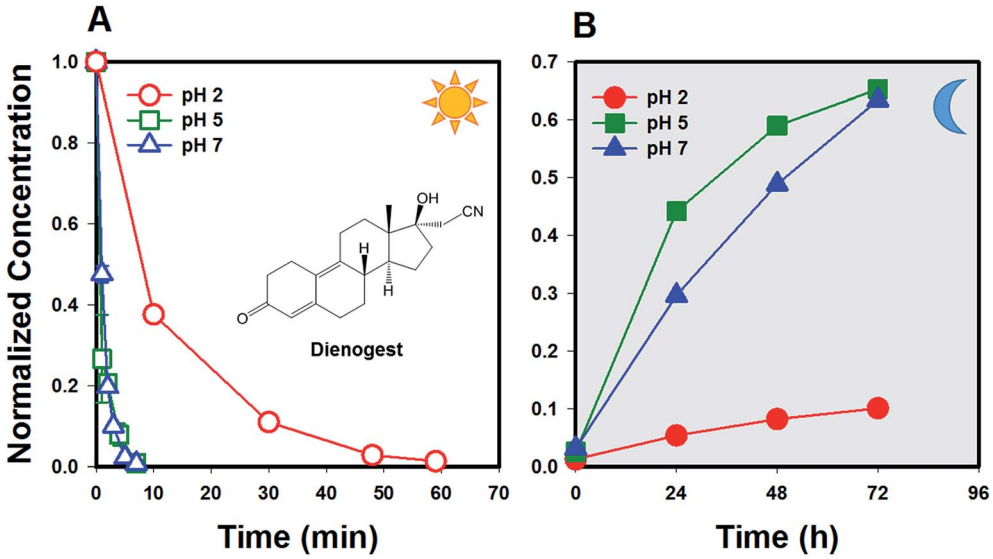

Fig. 1 Concentration of DNG (20 μM or ~6 mg L^{-1}) over time during (A) irradiation with simulated sunlight in direct photolysis experiments and (B) subsequent storage of photoproduct mixtures in the dark. Error bars represent one standard deviation from $n = 3$ replicates. If error bars are not visible, they are smaller than the symbol.

Primary transformation product identification

To assess how product distributions and yields evolved as a function of pH and duration of irradiance, we conducted photolysis reactions across a range of pH values (pH 2, 5 and 7) and photolysis times (up to 5 h). We note that while experiments at pH 7 and 5 have direct relevance to DNG fate in sunlit surface waters, the benefit of pH 2 experiments is their ability to evaluate acid-catalyzed processes that may influence DNG stability in moderately acidic surface waters (as we observed for the metabolites of trenbolone acetate).[10] Initial HPLC assessment revealed formation of complex mixtures containing multiple phototransformation products (see Fig. 2). As shown in Fig. 3, generally we observed differences in the yields and identity of major products as a function of pH and the extent of parent transformation, consistent with formation of some unstable or (photo) reactive products.

After initial assessment, analysis of the mixtures *via* HR-EI-TOFMS, HR-ESI-TOFMS, and NMR revealed that photolysis of DNG resulted in the formation of eight primary transformation products (*i.e.*, those observed to form during photolysis) across the range of pH values considered. Five of these product structures are shown in Fig. 4; we failed to isolate three primary products that remain unidentified (as shown in Fig. 2, one unknown was only observed at pH 2). Reactions at pH 2, 5, and 7 were then scaled-up, photolyzed for 2 hours (to DNG levels below our limit of analytical detection), extracted into organic solvent, and concentrated. Then, products were isolated *via* semi-preparative HPLC (see ESI† for a detailed account of fractionation and isolated masses). We note that ~1 h elapsed from the conclusion of irradiation to the time of product extraction from water, which likely explains our isolation of parent DNG (formed *via* reversion) and presumed secondary products (generated *via* ongoing thermochemical processes). For example, parent DNG was isolated at ~15% and 5% yield at pH 5 and 7, respectively, which we assume is the result of photohydrate dehydration during this 1 h interval.

The spectroscopic analyses that led to the identification of each product are discussed in greater detail below. To

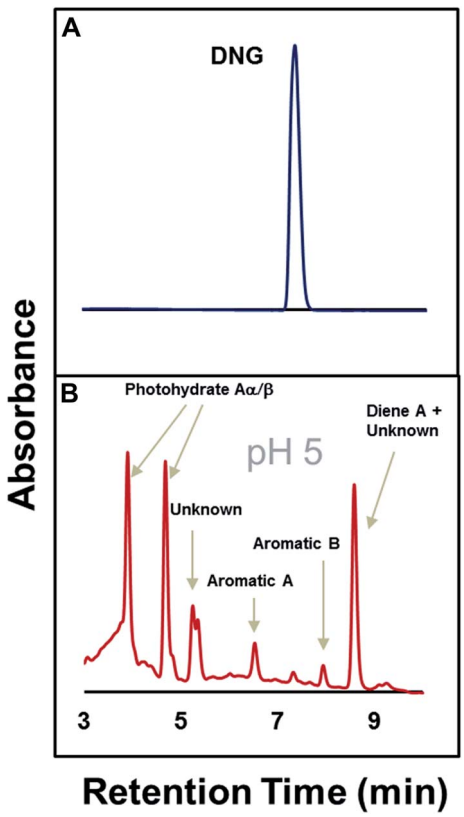

Fig. 2 LC-DAD trace of (A) DNG standard (λ_{det} 310 nm) and (B) a photoproduct mixture generated at pH 5 after irradiation of DNG for 2 h (λ_{det} 210 nm).

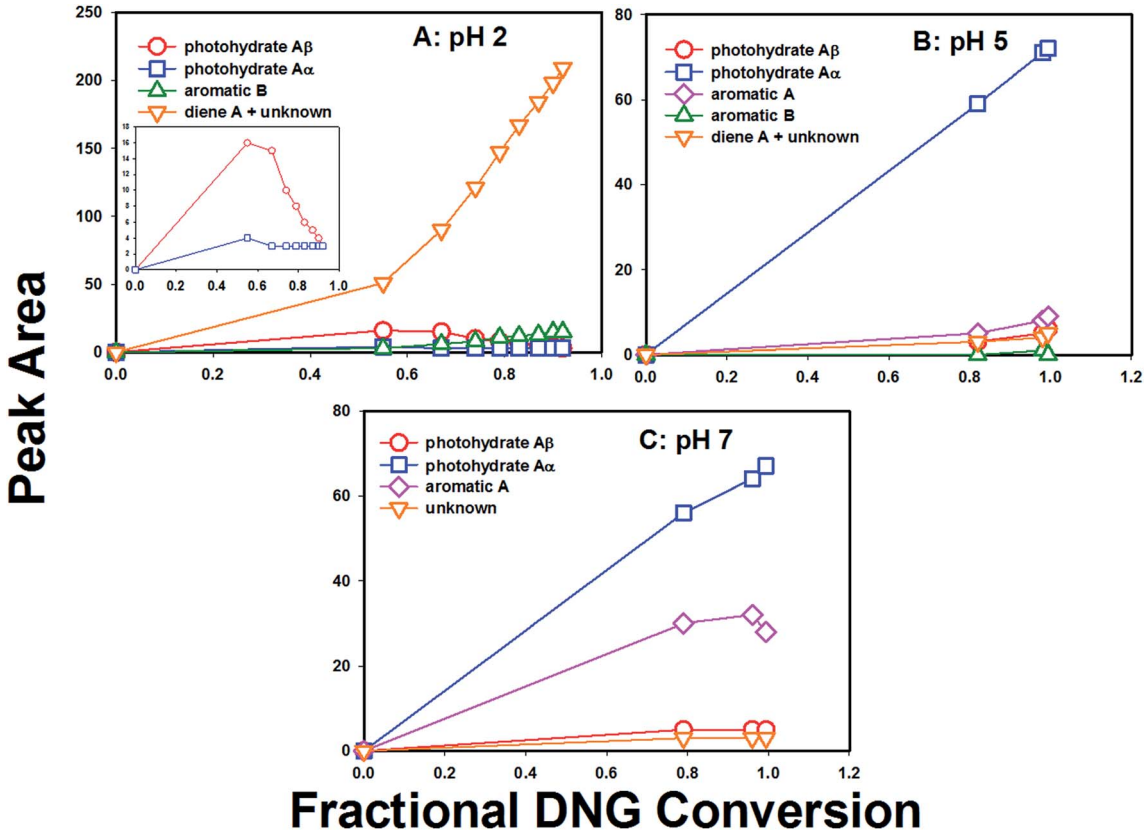

Fig. 3 Product distribution as a function of fractional DNG conversion during photolysis at (A) pH 2, (B) pH 5, and (C) pH 7, where the inset in panel A is a close-up of photohydrate Aβ and Aα formation at pH 2. While diene A and an as-yet unidentified compound co-eluted under the method used to collect these data (and hence they are shown as a combined peak area), the ratio of this unknown to diene A was approximately 1-to-8 at pH 2 and 1-to-1 at pH 5 based on yields from isolated product masses. Diene A was not observed at pH 7.

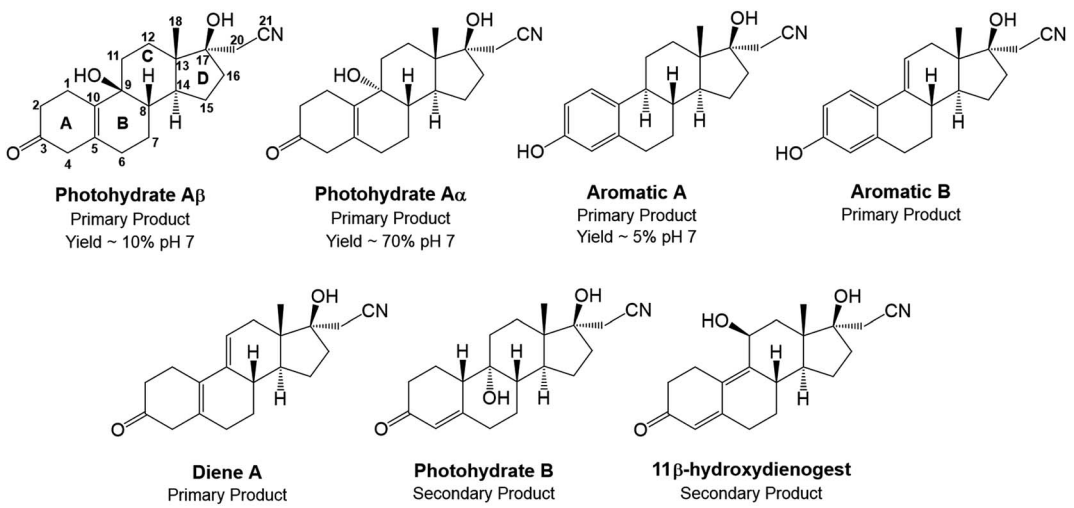

Fig. 4 Summary of primary and secondary transformation products identified during the direct photolysis of DNG across the range of pH values considered. Also provided are the yields for major products identified and quantified at pH 7.

accompany this discussion, ^{1}H and ^{13}C NMR data of parent DNG and all previously unreported transformation products are provided in Tables S1 and S2,† respectively. All HRMS spectra, NMR spectra, and energy minimized molecular models are presented in ESI Fig. S3–S38† in the order they are discussed below, beginning with parent DNG. In addition, full HMBC assignments of previously unreported products, HRMS and retention time data, and UV-vis spectra of all primary and

secondary products are shown in Tables S3, S4 and Fig. S39,† respectively. Lastly, we report isolated yields on a percent basis, which were calculated as mole product per mole parent consumed for all primary products isolated after a 2 h photolysis time at each pH value.

Photohydrate Aβ. HR-ESI-TOFMS analysis of pH 7 fraction 1 gave an $(M + H)^+$ ion at *m*/*z* 330.2068, corresponding to a product with the formula $C_{20}H_{27}NO_3$, indicative of the addition of water to parent DNG. ^{1}H NMR analysis revealed the disappearance of olefinic H-4, while UV analysis showed complete disruption of conjugation (λ_{max} < 220 nm). As shown in Fig. 5, the HMBC spectrum showed all expected correlations from H_3-18 to C-12, C-13, C-14 and C-17. H_2-12 showed key correlations to C-11 and an oxygenated carbon at 72.3 ppm (C-9, in addition to C-17). H_2-11 showed correlations to C-8, C-9, and an olefinic carbon at 130.6 ppm (C-10). As final structural confirmation of this product [*i.e.*, 9β,17α-dihydroxy-3-oxo-19-norpregna-5(10)-ene-21-nitrile], hereafter referred to as "Photohydrate Aβ", H_2-4 showed correlations to two olefinic carbons, one at 132.3 ppm (C-5) and the other at 130.6 ppm (C-10). Isolated yields of photohydrate Aβ were ∼15% and 10% at pH 5 and 7 respectively. We note that the stereochemical assignment of photohydrate Aβ is discussed in the following section concerning its diastereomer, which we refer to as "Photohydrate Aα".

Photohydrate Aα. HR-ESI-TOFMS of pH 7 fraction 2 gave an $(M + Na)^+$ ion at *m*/*z* 352.1869 and an $(M + K)^+$ ion at *m*/*z* 368.1617, corresponding to a product with the formula $C_{20}H_{27}NO_3$, again indicative of the addition of water to parent DNG. ^{1}H NMR analysis again revealed the disappearance of olefinic H-4 and UV analysis showed complete disruption of conjugation (λ_{max} < 220 nm). As shown in Fig. 5, the HMBC spectrum showed correlations from H_2-4 to two olefinic carbons, one at 134.1 ppm (C-5) and the other at 130.7 ppm (C-10). H_2-4 also showed correlations to a carbon at 30.3 ppm (C-6). H_2-6 showed correlations to the same two olefinic carbons (C-5 and C-10) and also to a carbon at 20.3 ppm (C-7). H_2-7 showed key correlations to an oxygenated carbon at 70.0 ppm (C-9) and only one olefinic carbon at 134.1 (C-5).

With the hydroxyl group at C-9 able to adopt two possible orientations (α or β), we concluded this product [*i.e.*, 9α,17α-dihydroxy-3-oxo-19-norpregna-5(10)-ene-21-nitrile], hereafter referred to as "Photohydrate Aα", to be the diastereomer of the previously isolated photohydrate Aβ. Isolated yields of photohydrate Aα were ∼15%, 50%, and 70% at pH 2, 5, and 7 respectively. Notably, photohydrate Aα had a much greater isolated yield than that of photohydrate Aβ in our experimental systems at pH 7 (∼10 mg compared to ∼1 mg, respectively), thus we assumed it to be the more thermodynamically stable conformer. To make stereochemical assignments, each structure was energy minimized using Spartan, with the α-hydroxy epimer calculated to be more stable (by ∼12 kJ mol^{-1}; see Fig. S15†). Thus, based on yields, we tentatively assigned photohydrate Aα as the 9α-hydroxy epimer.

Because relative photohydrate yields of trenbolone acetate metabolites have not always corresponded with relative thermodynamic stability,[10] NMR data was used to further validate these initial stereochemical assignments. The assignment of photohydrate Aα as the 9α-hydroxy epimer is supported by the downfield shifts of H_{ax}-12 and H-14 when compared to photohydrate Aβ (1.63 ppm *vs.* 1.52 ppm and 1.88 ppm *vs.* 1.51 ppm respectively), which can be ascribed to a 1,3-diaxial deshielding effect of the hydroxyl group on H_{ax}-12 and H-14.[28] Assignment of photohydrate Aβ as the 9β-hydroxy epimer is supported by the downfield shifts of H-8, H_{ax}-11 and H-18 when compared to photohydrate Aα (1.89 ppm *vs.* 1.58 ppm, 2.72 ppm *vs.* 2.00 ppm and 1.07 ppm *vs.* 0.96 ppm respectively), which could be ascribed to a deshielding effect of the hydroxyl group on H-8, H_{ax}-11 and H-18.

Aromatic A. HR-EI-TOFMS of pH 7 fraction 3 gave an $(M^{+\bullet})$ ion at *m*/*z* 311.1885, corresponding to a product with the formula $C_{20}H_{25}NO_2$, which is the same as parent DNG and

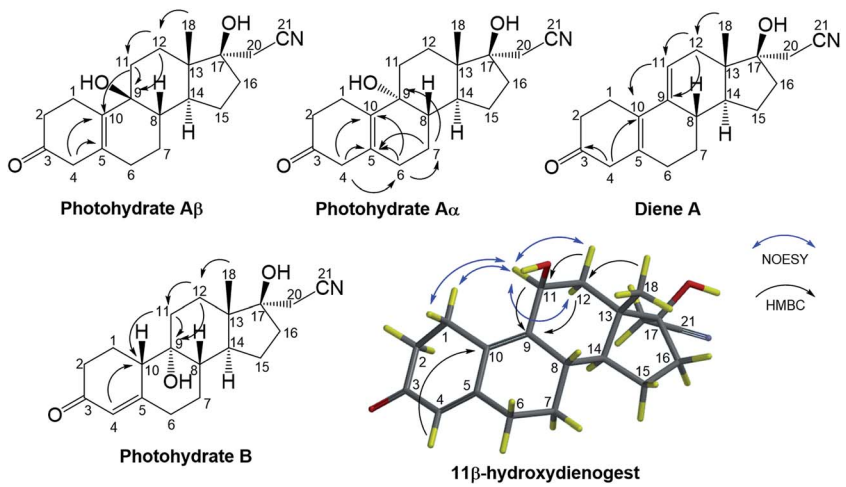

Fig. 5 Key HMBC correlations observed for three of the primary products (top): photohydrates Aα/β and diene A; and for the two isolated secondary transformation products (bottom): photohydrate B and 11β-hydroxydienogest. Key NOESY correlations also shown for 11β-hydroxydienogest.

suggests a possible rearrangement product. ^{1}H NMR analysis showed three aromatic proton signals with a 1,2,4-trisubstituted splitting pattern. The ^{1}H NMR, MS, and UV ($\lambda_{max} \sim 275$ nm) data for this product [*i.e.*, 3,17α-dihydroxy-19-norpregna-1,3,5(10)-triene-21-nitrile], hereafter referred to as "Aromatic A", all agree with that of known DNG metabolite, STS 433.[27] Aromatic A was isolated at ~5% yield at pH 7, and forms at trace levels at pH 5.

Aromatic B. HR-EI-TOFMS of pH 2 fraction 3 gave an $(M^{+\bullet})$ ion at *m*/*z* 309.1729, corresponding to a product with the formula $C_{20}H_{23}NO_2$, indicative of the loss of two protons from the parent DNG. ^{1}H NMR analysis showed three aromatic proton signals with a 1,2,4-trisubstituted splitting pattern and the emergence of a new olefinic multiplet at 6.11 ppm. The ^{1}H NMR, MS, and UV ($\lambda_{max} \sim 265$ nm) data for this product [*i.e.*, 3,17α-dihydroxy-19-norpregna-1,3,5(10),9(11)-tetraene-21-nitrile], hereafter referred to as "Aromatic B", all agree with that of known DNG metabolite STS 825,[27,29,30] which has also been identified as a product of DNG photolysis in organic solvent.[31] Aromatic B was isolated at ~20% yield at pH 2 and forms at trace levels at pH 5, suggesting the potential for formation only in mildly acidic surface waters.

Diene A. HR-ESI-TOFMS of pH 2 fraction 4.3 gave an $(M + H)^+$ ion at *m*/*z* 312.1953, corresponding to a product with the formula $C_{20}H_{25}NO_2$, which is the same as parent DNG and again suggests a possible rearrangement product. ^{1}H NMR analysis showed a broad olefinic singlet at 5.62 ppm and the emergence of four doublets at 2.05, 2.14, 2.86, and 2.90 ppm characteristic of two isolated methylene groups, while UV analysis showed some disruption of conjugation (λ_{max} hypsochromic shift of ~71 nm to 239 nm). The HMBC spectrum showed all of the expected correlations from H_3-18 to C-12, C-13, C-14, and C-17. The only other protons that showed correlations in the spectrum were H_2-20, which showed correlations to C-16, C-17, and C-21. HSQC analysis showed the isolated methylene doublets at 2.05/2.14 ppm to correlate to the same carbon at 33.0 ppm (C-12) that correlated to H_3-18 in the HMBC spectrum. COSY analysis showed a strong correlation from H_2-12 to the broad olefinic singlet at 5.62 ppm (H-11), suggesting a double bond at position C-9/C-11. HSQC data showed that the other isolated methylene doublets at 2.86/2.90 ppm correlated to a carbon at 44.9 ppm (C-4), which matches well with the corresponding data for H_2-4/C-4 of photohydrate Aβ (2.77/2.83 and 44.6 ppm respectively, previously discussed).

Due to decomposition of the first sample, another sample of the same compound (not completely purified) was analyzed by HMBC. As shown in Fig. 5, this spectrum showed key correlations from H-11 and H_2-4 to the same non-protonated olefinic carbon at 127.5 ppm (C-10), while H_2-4 also showed a correlation to a ketone carbon at 210.0 ppm (C-3). In addition, the spectrum showed key correlations from H_2-12 to C-11 and another olefinic carbon at 135.9 ppm (C-9). Given this information and that the UV spectrum showed some retained conjugation, the structure was assigned as the product [*i.e.*, 17α-hydroxy-3-oxo-19-norpregna-5(10),9(11)-diene-21-nitrile] hereafter referred to as "Diene A". Woodward–Fieser rules for calculating the λ_{max} of a transoid diene with five alkyl substituents agrees well with that of the experimental value (240 nm *vs.* 239 nm respectively).

A literature search of diene A revealed the compound to be a known intermediate in the synthesis of trienones, with ^{1}H NMR of the intermediate identical to that found for diene A.[32] As shown in Fig. S22,† after three days, ^{1}H NMR of isolated fraction 4.3 showed an approximately 1-to-0.85 mixture of diene A and 11β-hydroxydienogest (discussed later), suggesting the thermal rearrangement of diene A to the 11β-hydroxy product under dark conditions. This finding potentially explains why the first HMBC spectrum showed minimal correlations, as it was the last obtained in the series of experiments.

Isolated yields of diene A were ~40% and 5% at pH 2 and 5 respectively, once again indicating its formation is likely limited to mildly acidic surface waters. We note these yields are estimated assuming that any of the isolated 11β-hydroxydienogest was generated from diene A in the dark (*i.e.*, these yields include the mass associated with 11β-hydroxydienogest).

Secondary thermal rearrangement product identification

In addition to regeneration of the parent DNG, secondary thermal rearrangement products were occasionally observed after storage of the photolysis reaction mixtures in the dark (see Fig. 4). The spectroscopic analysis that led to the identification of two of these products are as follows:

Photohydrate B. After ~1 h, HR-ESI-TOFMS of pH 2 fraction 1 gave an $(M + H)^+$ ion at *m*/*z* 330.2070, corresponding to a product with the formula $C_{20}H_{27}NO_3$, indicative of DNG photohydration. With ^{1}H NMR analysis revealing the conservation of olefinic H-4 and UV analysis showing some disruption of conjugation (λ_{max} hypsochromic shift of ~62 nm to 248 nm), this led us to focus our attention on the C-9/C-10 double bond as the site for hydration. As shown in Fig. 5, the HMBC spectrum showed all expected correlations from H_3-18 to C-12, C-13, C-14 and C-17. H_2-12 showed key correlations to C-11 and an oxygenated carbon at 74.0 ppm (C-9, in addition to C-17). H_2-11 showed correlations to C-8 and an oxygenated carbon at 74.0 ppm (C-9) and a carbon at 47.5 ppm (C-10). As a final confirmation of the structure of this product [*i.e.*, 9α,17α-dihydroxy-3-oxo-19-norpregna-4-ene-21-nitrile], hereafter referred to as "Photohydrate B", H-4 showed a correlation to a carbon at 47.5 (C-10), but not the oxygenated carbon at 74.0 ppm (C-9). With the hydroxyl group at C-9 able to adopt two possible orientations (α or β), the structures of each were energy minimized using Spartan, and the α-hydroxy epimer was calculated to be more stable (~45 kJ mol^{-1}; see Fig. S31†). As further evidence of photohydrate B being the α-hydroxy epimer, H-14 is shifted considerably downfield when compared to the starting material (1.71 ppm *vs.* 1.27 ppm respectively), which could be ascribed to a 1,3-diaxial deshielding effect of the hydroxyl group on H-14.

11β-hydroxydienogest. HR-EI-TOFMS of pH 2 fraction 2 gave an $(M^{+\bullet})$ ion at *m*/*z* 327.1838, corresponding to a product with the formula $C_{20}H_{25}NO_3$, indicative of the substitution of a proton of DNG for a hydroxyl group. ^{1}H NMR analysis revealed the conservation of olefinic H-4 and a new broad doublet at

5.26 ppm, while UV analysis showed conservation of the dienone conjugation ($\lambda_{max} \sim 300$ nm). As shown in Fig. 5, the HMBC spectrum showed all expected correlations from H_3-18 to C-12, C-13, C-14 and C-17. H_2-12 showed key correlations to an oxygenated carbon at 79.0 ppm (C-11, in addition to C-17) and an olefinic carbon at 139.0 ppm (C-9). H-11 showed correlations to C-8 and two olefinic carbons at 139.0 ppm (C-9) and 134.0 ppm (C-10). As a final line of evidence of the structure of this product [*i.e.*, 11β,17α-dihydroxy-3-oxo-19-norpregna-4,9-diene-21-nitrile], hereafter referred to as "11β-hydroxydienogest", H-4 showed a correlation to the olefinic carbon at 134.0 (C-10), but not the olefinic carbon at 139.0 ppm (C-9).

With the C-11 hydroxyl group able to adopt two possible orientations (α or β), the structures of each were energy minimized using Spartan, and the β-hydroxy epimer was calculated to be more stable (~14 kJ mol^{-1}, see Fig. S38†). In further support of 11-hydroxydienogest being the β-hydroxy epimer, H_3-18 is shifted considerably downfield when compared to the starting material (1.16 ppm *vs.* 1.08 ppm respectively), which could be ascribed to a 1,3-diaxial deshielding effect of the hydroxyl group on H_3-18.

The final orientation of the C-11 hydroxyl group being the β-hydroxy epimer was assigned from the NOESY spectrum, which showed correlations between H-11 and H-1α/H-1β and H-12α/H-12β protons and the absence of correlations between H-11 and H-8 and H_3-18 (see Fig. 5). Energy minimized models show that for the β-hydroxy epimer the interatomic distances (IAD) between H-11 and H-1α/H-1β (2.035/2.847 Å) and H-12α/H-12β (2.361/2.499 Å) are shorter than for that of the α-hydroxy epimer (3.839/3.656 Å and 3.068/2.528 Å respectively). In addition, for the β-hydroxy epimer, the IAD between H-11 and H-8 (3.774 Å) and H-18 (3.947 Å) are much longer than for that of the α-hydroxy epimer (2.44 Å and 2.179 Å respectively), further supporting our assignment.

Transformation product stability

After photolysis, reaction product mixtures were stored in the dark and periodically analyzed *via* HPLC to monitor primary photoproduct stability and track formation of secondary thermal rearrangement products. In addition, a limited number of isolated products (*i.e.*, photohydrates Aα/β, photohydrate B, aromatic A, and 11β-hydroxydienogest) were reconstituted in water and then subsequently reanalyzed by HPLC to monitor their stability.

The two primary photohydrates (Aα and Aβ) generally undergo relatively rapid degradation in the dark (Fig. 6). Reanalysis of isolated samples of both products by HPLC resulted in a mixture of the primary photohydrate (Aα or Aβ), along with parent DNG and diene A. In addition, photohydrate Aα also showed photohydrate B in the mixture. We suspect that the two primary photohydrates (photohydrate Aα and Aβ) undergo either: (i) an acid- or base-catalyzed dehydration to regenerate DNG, or (ii) an acid-catalyzed dehydration to form diene A (see Fig. 7). Photohydrate Aα is also suspected to undergo (iii) a 1,3-sigmatropic rearrangement to produce secondary thermal photohydrate B (Fig. 7).

Pathway (ii) is illustrated in Fig. 3 for the pH 2 system, where after ~55% transformation of DNG there is a sharp increase in diene A formation, coinciding with loss of photohydrates Aα and Aβ. Likewise, process (iii) is highlighted in Fig. 6 for the pH 5 and 7 systems, where in the absence of light the primary photohydrate Aα undergoes degradation (*i.e.*, rearrangement) while the secondary photohydrate B is produced. We note that although this secondary photohydrate was not observed by HPLC in the pH 2 dark experiments, this product was isolated from the pH 2 photoreaction mixture, suggesting that it is formed at all pH values considered (*i.e.*, from pH 2 to 7). An isolated sample of photohydrate B was also suspended in water and reanalyzed by HPLC, which resulted in a mixture of the photohydrate and parent DNG. This suggests that photohydrate B can also undergo an acid- or base-catalyzed dehydration to regenerate DNG (see Fig. 7).

As previously discussed, diene A was found to undergo thermal rearrangement to 11β-hydroxydienogest in the dark. This process is demonstrated in Fig. 6 for the pH 2 and pH 5 systems, where thermal decay of diene A coincides with production of 11β-hydroxydienogest. HPLC analysis of an isolated sample of the 11β-hydroxy product after reconstitution in water (pH 2–7) showed relative stability at pH 5 and 7. At pH 2, however, it underwent rapid degradation to as-yet unidentifiable products (Fig. 6). This observation is also highlighted in Fig. 6 showing product evolution of the pH 2 and 5 reaction mixtures (top panels). The initial formation of 11β-hydroxydienogest is followed by relatively rapid degradation in the pH 2 system (where we have omitted signals associated with as-yet unidentified products for clarity). On the contrary, 11β-hydroxy product stability under pH 5 conditions is evident from its gradual and sustained formation over time.

As shown in Fig. 3, aromatic A was produced *via* irradiation at pH 5 and 7, and remained stable in the dark at these pH values (Fig. 6). We speculate that an as-yet unidentified intermediate, potentially a 10-hydroxy photohydrate, undergoes aromatization to form aromatic A. On the contrary, aromatic B was formed in the lower pH photolysis systems (pH 2 and 5), but also remained relatively stable when analyzing the mixtures under dark conditions and even doubled in concentration over time in the pH 5 system (Fig. 6). We again speculate that an as-yet unidentified intermediate leads to the formation of aromatic B.

Structural considerations influencing steroid reactivity and environmental fate

The results herein with DNG add to our growing body of evidence[10–14] that reversible photohydration represents a dominant fate pathway for steroids with π-bond conjugation across their A and B rings (*i.e.*, dienones) or A, B and C rings (*i.e.*, trienones). This π-bond conjugation both confers absorbance of wavelengths of light in the solar spectrum available at the earth's surface and drives photohydrate reversion to the thermodynamically preferred parent structure through gains in free energy associated with the dehydration reaction. Moreover, we have only observed reversion for steroids with linear s-*trans* conjugation (*e.g.*, trenbolone metabolites, dienedione and

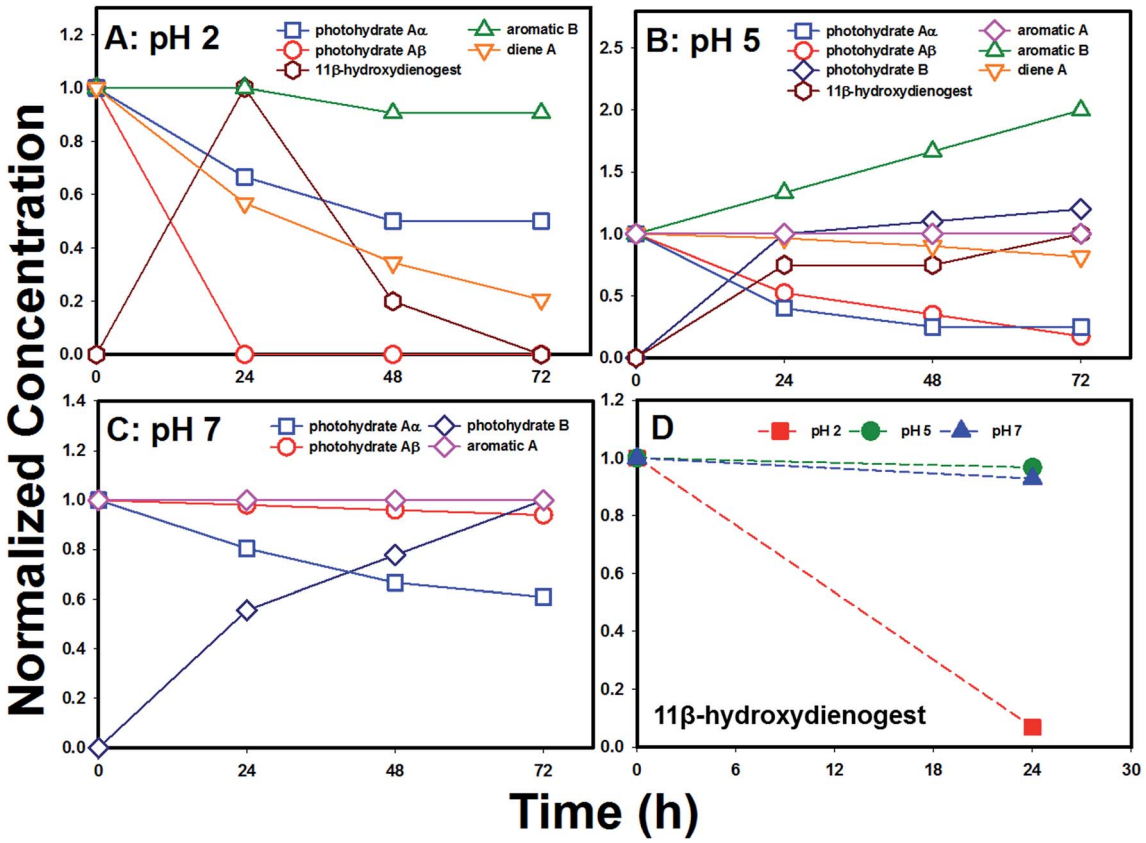

Fig. 6 Dark (thermal) stability of photoproduct mixtures at (A) pH 2, (B) pH 5, and (C) pH 7. Data in (D) show 24 h stability of isolated 11β-hydroxydienogest at pH 2, 5, and 7 (dashed lines are provided simply to help illustrate the observed trends).

photoisomers of altrenogest), rather than cross or linear s-*cis* conjugation. Indeed, additional photolysis studies conducted herein support this structural similarity among steroids prone to reversible photohydration; linearly s-*trans* conjugated gestrinone also undergoes reversion, but this phenomenon was not observed for several other linearly s-*cis* or cross-conjugated steroidal enones investigated (Fig. S40†). Among linearly s-*trans* conjugated enones, methylation within the conjugated π-system (*e.g.*, methylation at C-6 in melengestrol or melengestrol acetate) also seems to inhibit photoproduct to parent reversion (see Fig. S40† for structure).[12]

Ultimately, our observation of substantial DNG regeneration (~65% after 72 h at pH 7) in the dark implies its greater persistence in surface waters *via* the product-to-parent reversion cycle. We previously attributed the efficient regeneration of 17α-trenbolone, a trienone with a similar extent of regeneration (~55% after 72 h at pH 7), to the fast dehydration of its major photohydrate formed by water addition across C-4 (H^+) and C-5 (OH^-).[13] In contrast, we attributed the lower extent of 17β-trenbolone regeneration (~10% after 72 h at pH 7) to a slower rate of dehydration, because its major photohydrate incorporates water across its trienone moiety at C-4 (H^+) and C-12 (OH^-). A slower rate of dehydration would allow other reactions (*e.g.*, sequential water addition to yield more highly hydrated products) to predominate, consuming the photohydrate before extensive parent regeneration is possible.[13] However, the only secondary transformation pathway we observed in the DNG system was rearrangement of photohydrate Aα (the major product) to photohydrate B, another product also capable of reversion. Thus, for photohydrates generated by water addition across the dienone moiety [*i.e.*, C-4 (H^+) and C-9 (OH^-)], dehydration is sufficiently fast at pH 7 to promote DNG regeneration instead of sequential transformation to non-revertible products.

We anticipate the rate of dehydration, and thus the rate and extent of DNG regeneration, to be influenced by environmental factors. Although not explored explicitly herein, we have previously shown temperature to influence rate of reversion,[13] with more parent regrowth, and thus greater persistence, at higher water temperatures (*e.g.*, during summer months). Another environmental variable is pH; although we observed much less DNG regeneration under acidic conditions relative to neutral pH, dehydration of photohydrates likely proceeds *via* an acid-catalyzed E1 elimination of water. As with trenbolone acetate metabolites,[13] the stabilized carbocation intermediate produced after water loss is susceptible to rearrangement (*e.g.*, photohydrates Aα/β to diene A) as an alternative pathway to DNG regeneration. In very acidic pH regimes (*e.g.*, pH 2), carbocation rearrangement to promote diene A formation must occur faster than DNG regeneration, thus short-circuiting the reversion cycle and limiting reversion. In contrast, slightly acidic pH systems (*e.g.*, pH 5) behaved similarly to observations at neutral

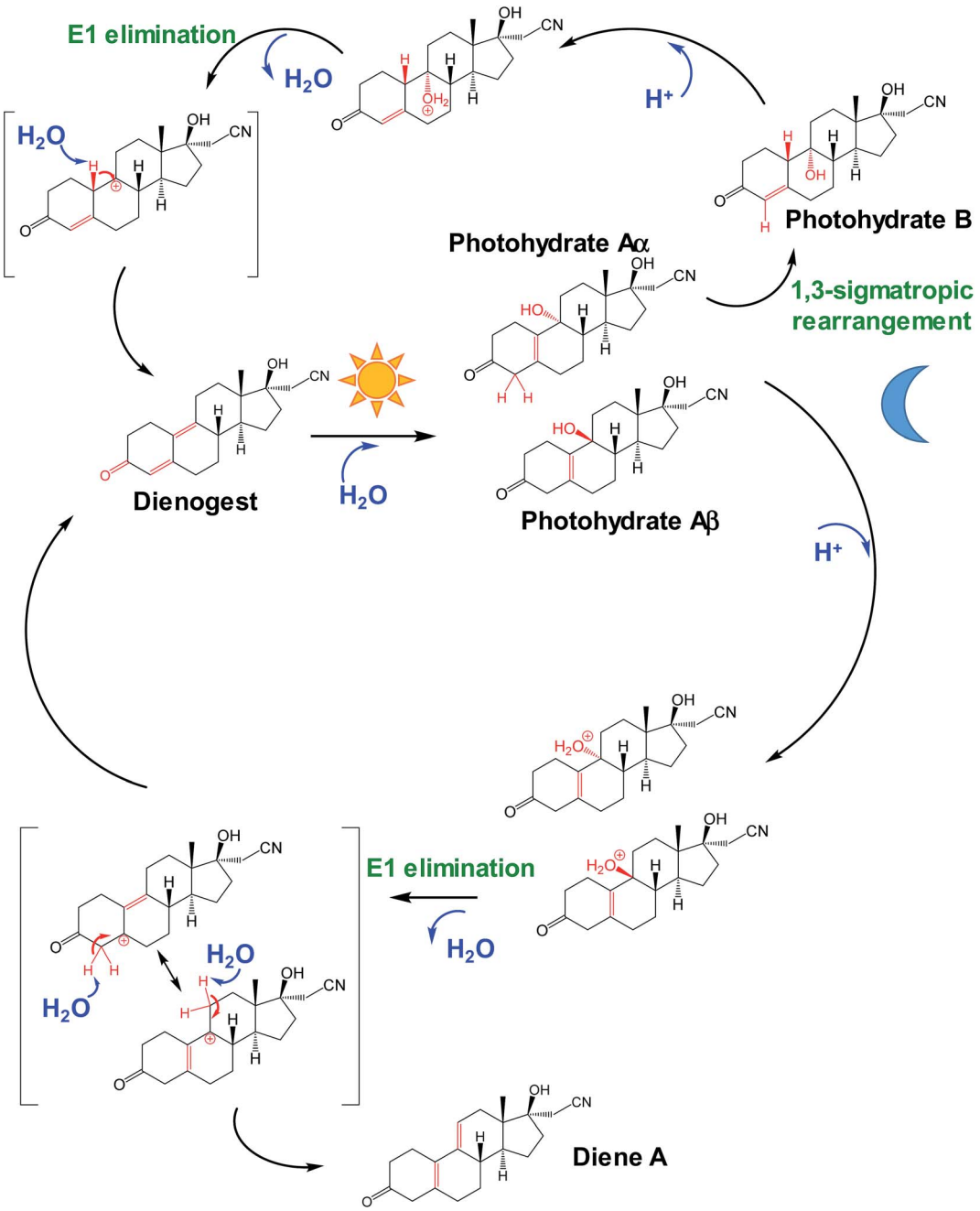

Fig. 7 Proposed reaction schematic for DNG direct photolysis and subsequent photoproduct transformations. DNG undergoes rapid photohydration yielding primary photohydrates Aα and Aβ. In the dark, photohydrate Aα can undergo a 1,3-sigmatropic rearrangement to produce secondary photohydrate B, or both primary photohydrates (Aα/β) can proceed through an acid-catalyzed E1 elimination resulting in either regeneration of parent DNG or formation of diene A *via* a resonance-stabilized carbocation intermediate. In addition, photohydrate B can proceed through an acid-catalyzed E1 elimination also resulting in regeneration of DNG.

pH (*i.e.*, ~65% DNG regeneration after 72 h), suggesting that the stability of the carbocation is not sufficient to facilitate rearrangement at these conditions.

Implications for product bioactivity and dienogest risk assessment

Beyond increased DNG persistence through product-to-parent reversion, our elucidation of product identities generally reveals conservation of steroidal structure, and thus the potential for retained or distinct bioactivity in DNG photoproducts. Although we did not conduct independent analysis of the isolated products' bioactivities, in many cases this information was available from prior studies. For example, 11β-hydroxydienogest is, in fact, a known DNG metabolite in microbes, mammals, and humans, previously identified as STS 749.[29,30,33,34] Prior investigations have revealed 11β-hydroxydienogest (STS 749) to exhibit trace progestogenic activity

equivalent to roughly 2% that of parent DNG.[33,34] Thus, its formation *via* thermal rearrangement of diene A presents a route to conserved progestogenic activity, particularly in slightly acidic surface waters (*e.g.*, pH 5) where 11β-hydroxydienogest (STS 749) exhibited stability over time.

Also notable are the two aromatic products we identified. A-ring aromatization of DNG has been previously reported for microbial DNG biotransformation and also can occur metabolically in humans and other mammals.[27,29,30] In our photochemical systems, we speculate that aromatic A (or STS 433) is generated from an initial photohydration step at C-10, followed by a fast thermal aromatization (*i.e.*, dehydration and enolization). A similar acid-catalyzed aromatization was previously described for the synthesis of estrone and estradiol.[35] We also speculate that aromatic B (or STS 825) is formed from an initial photochemically derived C-9/C-10 di-hydroxy intermediate, analogous to a species we isolated from 17β-trenbolone photolysis.[11] This intermediate could then proceed through a thermal dehydration of the 9-hydroxy substituent to set the C-9/C-11 olefin and a similar aromatization process as described for the formation of aromatic A.

Aromatization in the A-ring implies photochemical conversion of progestogenic DNG into estrogenic transformation products. Indeed, both aromatic products have previously been reported to exhibit estrogenic activity at ~30% that of the endogenous ligand 17β-estradiol.[27,33] Notably, this level of estrogenic activity is quite similar to that of estrone,[36] one of the most well-recognized steroidal transformation products in aquatic environments. It is well documented that low ng L^{-1} concentrations of estrogens can lead to feminization of male fish, altered oogenesis in females, and widespread ecosystem level effects (*e.g.*, decline in fish population and altered food web structure) upon exposure.[37–39] While the yields of these aromatic products were low in our experimental systems (*e.g.*, aromatic A was isolated at ~5% yield at pH 7), they represent non-revertible end products that are likely to accumulate over time through repeated cycling between DNG and its photohydrates. Thus, these minor, side reaction pathways may ultimately dominate the long-term fate of DNG, allowing estrogenic endpoints to accumulate over alternative reaction pathways.

Formation of these aromatic products may also result in biological endpoints beyond estrogen receptor (ER) affinity. Aromatic A is also reported to possess antiprogestational activity, ~6-fold more potent than DNG.[33] Aromatic B is also known to possess antigonadotropic activity (~2 times more potent than DNG), as well as antiprogestational activity (~4 times more potent than DNG), and also inhibits fertility (~75% as active as the abortive agent RU 486, known commercially as mifepristone).[33]

Finally, the bioactivity of photohydrates Aα/β is not known but merits further investigation. We have previously shown that photohydrates of trenbolone acetate metabolites exhibit bioactivity distinct from that of the parent compounds (*i.e.*, estrogenic *vs.* androgenic, respectively),[11] and thus speculate that DNG photohydrates also retain consequential bioactivity. Photohydrate stereochemistry, which we have elucidated here, should also influence bioactivity, as we have previously observed distinct bioactivity in photoproduct mixtures of 17α-trenbolone compared to 17β-trenbolone.[11]

Conclusions

For DNG, we have shown that transformation products are (i) a source of the parent (*via* reversion) and a pathway to persistence; (ii) known to retain PR activity and are contributors to mixture toxicity with probable adverse ecological impacts; and (iii) also have biological endpoints (ER *versus* PR) that are distinct from the parent. Moreover, DNG phototransformation is expected to occur readily in sunlit surface waters, because the absorbance of its dienone moiety overlaps with the wavelengths of sunlight available at earth's surface.

More work is needed to identify as-yet observed, but structurally unknown products. For example, we saw evidence of another potential aromatic compound that was observed to form across pH 2 to 7, and work is ongoing to elucidate its structure. In addition, although the presence or absence of oxygen in the experimental systems had little-to-no observable effect on the rate of DNG photolysis, results indicate oxygen may play a role in subsequent reduction-oxidation steps after initial photohydration. Thus, environmental factors including oxygen, presence of co-solutes, and extended diurnal cycling as a route to enriching initially minor end products, merit additional study. Finally, we recognize that this is a laboratory study and environmental occurrence of DNG and its phototransformation products is needed. We anticipate that outcomes herein related to the chemical reactivity and bioactivity endpoints of these species will help guide screening in systems where they would be expected to occur.

Collectively, our data indicate that we should no longer expect that the transformation of high potency pharmaceuticals equates with reduction of hazard to exposed organisms. More holistic approaches to risk assessment of such high potency environmental contaminants, especially those with the potential to exhibit diverse biological endpoints, are needed to accurately assess the fate and effects of such emerging pollutant classes and their bioactive transformation products.

Conflicts of interest

There are no conflicts to declare.

Acknowledgements

Support for this work from NSF (CBET-1335711 and CHE-1609791) and the University of Iowa (UI; Research Fellowship to NCP) is gratefully acknowledged. We would like to thank Dr Santhana Velupillai of the UI Central NMR Facility and Dr Lynn Teesch and Mr Vic Parcell of the UI High Resolution Mass Spectrometry Facility for their support in product analysis. We would also like to thank Dr Shen Qu formerly of the UI and Dr Chris Jeffrey of the University of Nevada, Reno for their assistance on DNG photolysis experiments. We would also like to thank the three anonymous reviewers for their constructive feedback on our work.

References

1 Environmental Protection Agency, Contaminant Candidate List, https://www.epa.gov/ccl, accessed May 3, 2017.
2 H. Segner, A. Casanova-Nakayama, R. Kase and C. R. Tyler, Impact of environmental estrogens on fish considering the diversity of estrogen signaling, *Gen. Comp. Endocrinol.*, 2013, **191**, 190–201.
3 M. G. Bertram, M. Saaristo, J. B. Baumgartner, C. P. Johnstone, M. Allinson, G. Allinson and B. B. M. Wong, Sex in troubled waters: Widespread agricultural contaminant disrupts reproductive behaviour in fish, *Horm. Behav.*, 2015, **70**, 85–91.
4 E. F. Orlando and L. E. Ellestad, Sources, concentrations, and exposure effects of environmental gestagens on fish and other aquatic wildlife, with an emphasis on reproduction, *Gen. Comp. Endocrinol.*, 2014, **203**, 241–249.
5 G. D. Jones, P. V. Benchetler, K. W. Tate and E. P. Kolodziej, Trenbolone acetate metabolite transport in rangelands and irrigated pasture: observations and conceptual approaches for agro-ecosystems, *Environ. Sci. Technol.*, 2014, **48**(21), 12569–12576.
6 M. Safholm, A. Ribbenstedt, J. Fick and C. Berg, Risks of hormonally active pharmaceuticals to amphibians: a growing concern regarding progestagens, *Philos. Trans. R. Soc., B*, 2014, **369**(1656), 7.
7 T. E. Frankel, M. T. Meyer, D. W. Kolpin, A. B. Gillis, D. A. Alvarez and E. F. Orlando, Exposure to the Contraceptive Progestin, Gestodene, Alters Reproductive Behavior, Arrests Egg Deposition, and Masculinizes Development in the Fathead Minnow (Pimephales promelas), *Environ. Sci. Technol.*, 2016, **50**(11), 5991–5999.
8 V. Kumar, A. C. Johnson, A. Trubiroha, J. Tumova, M. Ihara, R. Grabic, W. Kloas, H. Tanaka and H. K. Kroupova, The Challenge Presented by Progestins in Ecotoxicological Research: A Critical Review, *Environ. Sci. Technol.*, 2015, **49**(5), 2625–2638.
9 E. Bratoeff, M. Cabeza, E. Ramirez, Y. Heuze and E. Flores, Recent advances in the chemistry and pharmacological activity of new steroidal antiandrogens and 5 alpha-reductase inhibitors, *Curr. Med. Chem.*, 2005, **12**(8), 927–943.
10 J. Baltrusaitis, E. V. Patterson, M. O'Connor, S. Qu, E. P. Kolodziej and D. M. Cwiertny, Reversible photohydration of trenbolone acetate metabolites: mechanistic understanding of product-to-parent reversion through complementary experimental and theoretical approaches, *Environ. Sci. Technol.*, 2016, **50**, 6753–6761.
11 E. P. Kolodziej, S. Qu, K. L. Forsgren, S. A. Long, J. B. Gloer, G. D. Jones, D. Schlenk, J. Baltrusaitis and D. M. Cwiertny, Identification and Environmental Implications of Photo-Transformation Products of Trenbolone Acetate Metabolites, *Environ. Sci. Technol.*, 2013, **47**(10), 5031–5041.
12 S. Qu, E. P. Kolodziej and D. M. Cwiertny, Phototransformation rates and mechanisms for synthetic hormone growth promoters used in animal agriculture, *Environ. Sci. Technol.*, 2012, **46**, 13202–13211.
13 S. Qu, E. P. Kolodziej, S. A. Long, J. B. Gloer, E. V. Patterson, J. Baltrusaitis, G. D. Jones, P. V. Benchetler, E. A. Cole, K. C. Kimbrough, M. D. Tarnoff and D. M. Cwiertny, Product-to-parent reversion of trenbolone: unrecognized risks for endocrine disruption, *Science*, 2013, **342**(6156), 347–351.
14 K. H. Wammer, K. C. Anderson, P. R. Erickson, S. Kliegman, M. Moffatt, S. M. Berg, J. A. Heitzman, N. C. Pflug, K. McNeill, D. Martinovic-Weigelt, R. Abagyan, D. M. Cwiertny and E. P. Kolodziej, Environmental photochemistry of altrenogest: photoisomerization to a bioactive product with increased environmental persistence *via* reversible photohydration, *Environ. Sci. Technol.*, 2016, **50**, 7480–7488.
15 D. M. Cwiertny, S. A. Snyder, D. Schlenk and E. P. Kolodziej, Environmental Designer Drugs: When Transformation May Not Eliminate Risk, *Environ. Sci. Technol.*, 2014, **48**(20), 11737–11745.
16 B. I. Escher and K. Fenner, Recent advances in environmental risk assessment of transformation products, *Environ. Sci. Technol.*, 2011, **45**, 3835–3847.
17 J. L. Chen, S. Ravindran, S. Swift, L. J. Wright and N. Singhal, Catalytic oxidative degradation of 17 alpha-ethinylestradiol by Fe-III-TAML/H2O2: Estrogenicities of the products of partial, and extensive oxidation, *Water Res.*, 2012, **46**(19), 6309–6318.
18 J. Y. Hu, S. J. Cheng, T. Aizawa, Y. Terao and S. Kunikane, Products of aqueous chlorination of 17 beta-estradiol and their estrogenic activities, *Environ. Sci. Technol.*, 2003, **37**(24), 5665–5670.
19 N. C. Pflug, A. Kupsco, E. P. Kolodziej, D. Schlenk, L. M. Teesch, J. B. Gloer and D. M. Cwiertny, Formation of bioactive transformation products during glucocorticoid chlorination, *Environ. Sci.: Water Res. Technol.*, 2017, **3**, 450–461.
20 Y.-Y. Yang, T. Borch, R. B. Young, L. D. Goodridge and J. G. Davis, Degradation Kinetics of Testosterone by Manure-Borne Bacteria: Influence of Temperature, pH, Glucose Amendments, and Dissolved Oxygen, *J. Environ. Qual.*, 2010, **39**, 1153–1160.
21 J. S. Stevenson and D. L. Davis, Estrous synchronization and fertility in gilts after 14- or 18-day feeding of altrenogest beginning at estrus or diestrus, *J. Anim. Sci.*, 1982, **55**, 119–123.
22 M. Dura, J. E. Tilton, A. Ziecik and G. L. Williams, Use of altrenogest alone or in combination with PMSG to control the preovulatory LH surge in gilts, *Animal Reproductive Science*, 1987, **14**, 147–155.
23 L. M. K. Pallapothu, N. Batta, R. K. Pigili and R. P. Yejella, A simple, rapid and sensitive liquid chromatography-tandem mass spectrometry method for the determination of dienogest in human plasma and its pharmacokinetic applications under fasting, *Biomed. Chromatogr.*, 2015, **29**(2), 194–201.
24 A. L. Nelson, An update on new orally administered contraceptives for women, *Expert Opin. Pharmacother.*, 2015, **16**(18), 2759–2772.

25 M. Oettel and A. Kurischko, STS 557, a new orally active progestin with antiprogestational and contragestational properties in rabbits, *Contraception*, 1980, **21**, 61–75.
26 R. H. Foster and M. I. Wilde, Dienogest, *Drugs*, 1998, **56**(5), 825–833.
27 G. Kaufmann, H. Dautzenberg, H. Henkel, G. Muller, T. Schafer, B. Undeutsch and M. Oettel, Nitrile hydratase from Rhodococcus erythropolis: Metabolization of steroidal compounds with a nitrile group, *Steroids*, 1999, **64**(8), 535–540.
28 J. R. Hanson, *Natural products: the secondary metabolites*, 2003.
29 G. Hobe, R. Schon, G. Frankenberg, W. Schade and K. Schubert, Urinary metabolites of the new progestagen STS 557 in the dog and rat, *Steroids*, 1983, **41**(1), 23–33.
30 K. Schubert, G. Hobe, G. Kaufmann, G. Schumann, K. Wehrberger and C. Horhold, Studies on the biotransformation of STS 557, *Exp. Clin. Endocrinol.*, 1983, **81**(2), 168–174.
31 T. T. Nguyen, *Syntheses and photo-reactivity of chromene natural products and photo-degradation of steroidal hormones*, University of Nevada, Reno, 2015.
32 G. Teichmuller and G. Muller, Process for the production of unsaturated 17a-cyanomethyl-17b-hydroxy steroids, *US pat.*, 5438134, 1995.
33 M. Oettel, G. Kaufmann and A. Kurischko, The endocrinological profile of metabolites of the progestin dienogest, *Pharmazie*, 1993, **48**(7), 541–545.
34 G. Kaufmann, J. Schlegel, B. Eychenne and K. Schubert, Receptor binding of STS 557, *Exp. Clin. Endocrinol.*, 1983, **81**(2), 222–227.
35 P. Kocovsky and R. Baines, Stereoelectronically controlled, thallium (III)-mediated C-19 degradation of 19-hydroxy steroids. An expedient route to estrone and its congeners *via* 19-nor-10β-hydroxy intermediates, *J. Org. Chem.*, 1994, **59**, 5439.
36 K. L. Thorpe, R. I. Cummings, T. H. Hutchinson, M. Scholze, G. Brighty, J. P. Sumpter and C. R. Tyler, Relative potencies and combination effects of steroidal estrogens in fish, *Environ. Sci. Technol.*, 2003, **37**, 1142–1149.
37 K. A. Kidd, P. J. Blanchfield, K. H. Mills, V. P. Palace, R. E. Evans, J. M. Lazorchak and R. W. Flick, Collapse of a fish population after exposure to a synthetic estrogen, *Proc. Natl. Acad. Sci.*, 2007, **104**(21), 8897–8901.
38 K. A. Kidd, M. J. Paterson, M. D. Rennie, C. L. Podemski, D. L. Findlay, P. J. Blanchfield and K. Liber, Direct and indirect responses of a freshwater food web to a potent synthetic oestrogen, *Philos. Trans. R. Soc., B*, 2014, **369**, 1–11.
39 L. S. Lee, N. Carmosini, S. A. Sassman, H. M. Dion and M. S. Sepulveda, Agricultural contributions of antimicrobials and hormones on soil and water quality, *Adv. Agron.*, 2007, **93**, 1–67.
40 G. Hobe, R. Schon, M. Hajek, K. Undisz and A. Hartl, Studies on the hydrogenation of the progestagen dienogest *in vivo* and *in vitro* in the female rabbit, *Steroids*, 1998, **63**, 393–400.

